MedChemComm

Accepted Manuscript

This is an *Accepted Manuscript*, which has been through the Royal Society of Chemistry peer review process and has been accepted for publication.

Accepted Manuscripts are published online shortly after acceptance, before technical editing, formatting and proof reading. Using this free service, authors can make their results available to the community, in citable form, before we publish the edited article. We will replace this *Accepted Manuscript* with the edited and formatted *Advance Article* as soon as it is available.

You can find more information about *Accepted Manuscripts* in the Information for Authors.

Please note that technical editing may introduce minor changes to the text and/or graphics, which may alter content. The journal's standard Terms & Conditions and the Ethical guidelines still apply. In no event shall the Royal Society of Chemistry be held responsible for any errors or omissions in this *Accepted Manuscript* or any consequences arising from the use of any information it contains.

ROYAL SOCIETY OF CHEMISTRY

www.rsc.org/medchemcomm

Journal Name

COMMUNICATION

One Small Molecule as Theranostic Agent: Naphthalimide Dye for Subcellular Fluorescent Localization and Photodynamic Therapy *in vivo*†

Received 00th January 20xx,
Accepted 00th January 20xx

DOI: 10.1039/x0xx00000x

www.rsc.org/

Lei Zhang,[a,‡] Kecheng Lei,[b,‡] Jingwen Zhang,[a] Wenlin Song,[a] Yuanhong Zheng,[b] Shaoying Tan,[a] Yuwei Gao,[b] Yufang Xu,[a,*] Jianwen Liu[b,*] and Xuhong Qian[a,*]

A novel single and small molecular theranostic agent (1a**)** based on a naphthalimide dye has been developed and characterized. The agent (1a) displays excellent fluorescence for cell imaging (fluorescent quantum yields of 0.81) and photodynamic effects for therapeutic (micromolar inhibition efficacy *in vitro* towards a broad spectrum of tumor models and anticancer treatment *in vivo* on A375 tumor xenograft models). This provides a new approach for simultaneous improvements of two directions of a small molecule as theranostic agent, which usually were in conflict with each other for the most and traditional theranostic agents.

Theranostic, executing diagnostic imaging and treatment simultaneously, has drawn extensive attentions in the development of personalized therapy.[1] During the past dozen years, theranostic agents have been fully developed and divided into two separate parts: (1) Complexes that assemble therapeutic and imaging units on various biomaterials including polymers, micelles, nanoparticles and protein conjugates. These agents exert additional capabilities like targeting, solubility, biocompatibity and even higher diagnostic accuracy.[2] (2) Large molecules performed by conjugating several functional components including drugs, imaging units, targeting groups and quenchers with covalent linkers. These molecules can readily distribute to target regions and function directly or activated by intracellular environment such as pH, enzymes or light.[3] Both of the agents have displayed diverse efficacy for application, however, the large sizes and intricate structures also bring some challenges, such as preparation, delivery, cellular internalization and therapeutic effects.[1b, 4]

Photosensitizers are a kind of molecules widely used in photodynamic therapy (PDT), and most of them show some extent of fluorescence or phosphorescence, which means they are able to achieve theranostic on one single nucleus.[5] Singh and co-workers have reviewed a series of glycosylated porphyrin and phthalocyanine-based photosensitizers and discussed their abilities for therapeutics and diagnositics.[6] Among those structures, chlorins (fluorescent quantum yield of 0.18) is described as a considerable candidate as theranostic agent. In recent researches, a large amount of newly-developed photosensitizers[7] have been designed and characterized with improving efficacy for PDT, however, the imaging properties of photosensitizers themselves did not seem to be promised, as these two functions or performances usually conflict each other, which is difficult to be adjusted or balanced. Thus, to discover some newly photosensitive candidates beyond the conflict or balance between the two functions, which possess both sufficient diagnosis and biological effects for photosensitive theranostic research is of most importance.

1,8-naphthalimides are recognized as superior fluorophores and chemotherapeutic drugs for anticancer research during the past decades.[8] They feature simple and stable structures, excellent optical properties of photostabilities, large stokes shift, high fluorescent quantum yields and extinction coefficients as fluorescent compounds

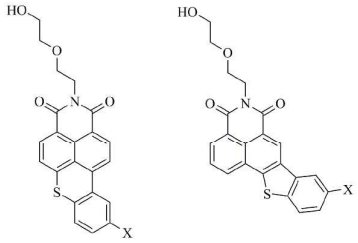

Fig.1 The structures of **1a-1d**

[a]*State Key Laboratory of Bioreactor Engineering, Shanghai Key Laboratory of Chemical Biology, School of Pharmacy, East China University of Science and Technology, Shanghai 200237, China. Phone/Fax: Tel: 86-21-64251399, Fax: 86-21-64252603; E-mail: xhqian@ecust.edu.cn,yfxu@ecust.edu.cn;*

[b] *State Key Laboratory of Bioreactor Engineering, Shanghai Key Laboratory of New Drug Design, School of Pharmacy, East China University of Science and Technology, Shanghai 200237, China. E-mail: liujian@ecust.edu.cn.*

‡ Authors contributed equally to this work.

† The authors declare no competing interests.

Electronic Supplementary Information (ESI) available: Experimental, synthetic, UV and PL spectrum,Fluorescent confocal microscopy, ^{1}H NMR, ^{13}C NMR, HRMS spectra, and bioassay details. See DOI: 10.1039/b000000x/

and considerable safety in drug discoveries.[9] It should be considered as a new scaffold for the derivation of novel theranostic agents. On the other hand, it was well-known that heavy atom effect, e.g. iodine, is gaining increasing attention in photosensitizer design,[10] due to its ability in increasing intersystem crossing (ISC) rate and improving the generation of singlet oxygen for photosensitive effects.[11] However, such strategy will dramatically decrease the fluorescent quantum yield and lifetime of singlet excited states of fluorescent dye, which is not helpful for the fluorescent cellular locallization.

In this sense, based on our previous work, we selected two thio-heterocyclic fused naphthalimides, **1c** and **1d**,[12] which had acceptable antitumor activities or favourable fluorescent properties, as new scaffolds of theranostic agents and employ bromine atom, which possess moderate heavy atom effect, as a proper heavy atom to realize fluorescence and PDT simultaneously (Fig. 1, **1a** and **1b**),[7c] besides, we chose diglycolamine to improve the solubility of final compounds **1a-d**. The synthetic routes were presented in Scheme.1. 4-bromo-3-nitro-1,8-naphthalic anhydride (**2**) was treated with benzenethiol or 4-bromobenzenethiol in ethanol at reflux to obtain **3a-b**. Then the nitryls on derivatives **3a-b** was reduced to amino group (**4a-b**) with stannous chloride dihydrate and hydrochloric acid. The final products (**1a-1b** and **1c-1d)** could be directly prepared through one-pot syntheses from **4a-b** after diazotization, cyclization and imidization.

Compared with the five-membered heterocyclic molecules **1b** and **1d**, the absorption maxima of **1a** and **1c** were red-shift to around 465 nm (Table 1, Fig. S1), and the fluorescent quantum yields were calculated to be 0.81 and 0.90, respectively. It meaned they were brighter than most of the conventional and new-structural photosensitizers,[13] which was beneficial to enhance the imaging performance of these photosensitive compounds. Then, as phototherapeutic agents, the singlet oxygen generation of **1a** and **1c** were determined with DPBF in aerated acetonitrile. Since the absorption curves of **1b** and **1d** overlapped with DPBF (410 nm), the data of these two compounds were not identified here. Upon irradiation of 470 nm monochromatic light (the absorption maximums of tested compounds), the absorbance values of DPBF (410 nm) decreased with the extended irradiation time, and singlet oxygen quantum yields were obtained with Methylene Blue (MB) as control (Table 1). In accordance with our hypothesis, **1a** showed a relatively more efficient quantum yield than **1c** due to the proper heavy atom effect of bromine.

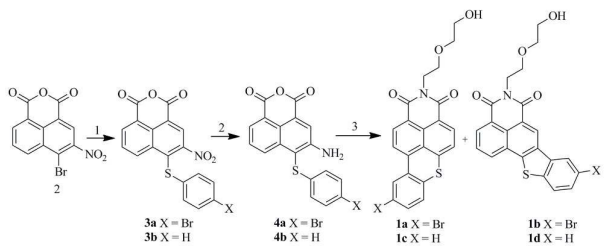

Scheme 1. Chemical synthesis of **1a-1d**. 1, thiophenol derivatives, ethanol, reflux, 5 h; 2, $SnCl_2{\cdot}2H_2O$, conc. HCl, 85 °C, 3 h; 3, (I) $NaNO_2$, conc. H_2SO_4, HOAc, 0 °C, 1 h; (II) $CuSO_4$, H_2O, HOAc, reflux, 6 h and then (III) diglycolamine, ethanol, 50 °C, 3 h.

Table 1. Optical properties and MTT assays (in MCF-7) of **1a-1d**.

	λ_{Abs} (nm)	λ_{Em} (nm)	ε (M^{-1} cm^{-1})	Φ_F[a]	Φ_Δ[b]	IC_{50} (μM) **0 J/cm²**	**28.8 J/cm²**
1a	465	520	16560	0.81	0.12	>50	2.65
1b	383	422	13710	0.018	nd	>50	18.50
1c	463	515	11730	0.90	0.054	18.20	1.40
1d	380	433	12830	0.13	nd	18.80	11.40
HpD						>50	4.20

[a] All data were measured in ethanol. [b] All data were measured in acetonitrile.

The photocytotoxicity of **1a-1d** on MCF-7 cells were evaluated through MTT assays (Fig. S2a and Table 1). The cells were treated with compounds for 48 hours and data were obtained after laser irradiation for a dose of 28.8 J/cm² within 20 min. **1a** presented a pronounced photocytotoxic activity with an IC_{50} value of 2.65 μM, which was even better than HpD of 4.2 μM. Moreover, there was an apparent difference of cytotoxicity between irradiated and non-irradiated conditions (dark toxicity was above 50 μM), indicating the photo-triggered toxicity of **1a**. **1c** also gave a valid IC_{50} toxicity of 1.4 μM after irradiation, but unfortunately, the toxicity in dark environment was also strong, what was supposed to be the DNA intercalative effect.[12b] By comparison, **1b** and **1d** showed less efficient IC_{50} toxicity in both cases. After that, we investigated the photo-cytotoxicity of **1a** on several cancer cells (Fig. S2b). **1a**-mediated PDT caused dose-dependent cell death by laser irradiation and showed the broad spectrum anticancer activities for MCF-7 (human breast cancer line), MKN45 (human gastric cancer line), HCT116 (human colon cancer line) and A375 (human melanoma cancer line). In view of the visible-light absorption property of 1a-induced PDT and the depth of tissue penetration, we chose A375 cell

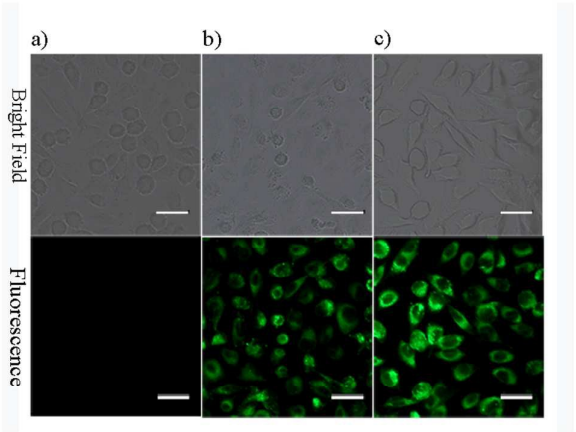

Fig. 2 Fluorescence imaging of **1a** in A375 cells. a) blank; b) The cells were loaded with **1a** for 48 hour; c) The cells were loaded with **1a** for 48 hour and then laser irradiation at a light dose of 28.8 J/cm². Bars: 15 μm

as an ideal subject for cell imaging and in vivo experiment, since A375 was a superficial skin cancer line which was feasible under photo-radiation on skin by visible light.

We then studied the intracellular imaging efficiency of **1a** during therapy process on A375 cells. **1a** could easily pass through cell membrane and visualize cells before or after treatment (Fig. 2). The changed cell morphology was obviously observed after PDT by fluorescence manner. Subsequently, to explore subcellular localization of **1a**, commercial fluorescent probes of mitochondria, endoplasmic, reticulum, lysosomes and nucleus were applied severally for co-localization inside cells by fluorescence confocal microscopy (Fig. S3). The merged images demonstrated that **1a** mainly accumulated in mitochondria rather than any other organelles. These phenomena indicated that on the premise of ensuring the anti-cancer therapeutic effect, **1a** could optimize the imaging results for monitoring process of therapy.

The effect of tumor growth inhibition by **1a** was then evaluated *in vivo* experiments. A375 cells were subcutaneously inoculated inside mice, and the tumor bared mice were divided into three groups: control group (no laser and no **1a**), medicine group (no laser but **1a**-treated) and PDT group (laser irradiation and **1a**-treated). After 21 days treatment (Fig. 3a), the tumor size increased to about 3.00±0.40 times as large as original size in medicine group and about 4.31±0.38 times in control group, however, only about 0.5-fold increase was measured in PDT group (Fig. 3b and 3c(B)), suggested that **1a**-PDT could significantly inhibit the growth of tumor xenograft. During this study, we also monitored the body weight of all mice, and no significant change was observed in all experimental sessions (Fig. 3c (A)). Besides, the H&E staining images of slices harvested from different tissues demonstrated that only in tumor slices, severely tissue lesions were obviously recognized in PDT group and a certain extent changes were found in medicine group (Fig. S4). These phenomena indicated that **1a** effectively caused tumor suppression after laser irradiation with negligible side effects.

Furthermore, on the basis of mitochondrial location behaviour of fluorescence confocal imaging, a series of confirmatory trials on the detection of **1a**-PDT induced cell apoptosis were designed and conduced in living cells and tissues. We firstly evaluated the intracellular reactive oxygen species (ROS) generation after PDT treatment (Fig. 4a). The intracellular ROS level reached the maximum after 4 hours and followed by a decrease to basal level within 12 hours. The excess ROS around mitochondria was supposed to cause oxidative stress and activate the pathway of apoptosis.[14] To verify this, western blot analysis was utilized to detect the expression of apoptosis-associated enzymes on mitochondrial pathway (Fig. 4b). Caspase 3 was one of the most important downstream protein-cleavage enzymes, which was found to be over-expression after PDT treatment, the cleaved-caspase 3 and cleaved-PARP (PARP was the major substrate of caspase 3) increased in a time-dependent manner due to activation of this apoptosis pathway.[15] Immunohistochemical analysis of tumor tissues also proved that cells apoptotic index increased with cleaved-caspase 3 expression after **1a**-PDT (Fig. S5). Finally, apoptotic effect of **1a**-PDT was determined by Hochest staining (Fig. 4c). Nuclear condensation and fragmentation, apoptotic bodies (bright blue) were clearly observed in PDT group after 12 hours, and the TUNEL staining also showed a large scale of TUNEL-positive apoptotic cells in tumor tissues, suggested a significantly high apoptotic rate after **1a**-PDT treatment (Fig. S6). Besides, all control groups and medicine groups in above experiments displayed negative responds. These evidences substantiated the possible mechanism of **1a**-induced PDT treatment that the massive intracellular ROS of **1a**-PDT regulated the activation of mitochondrial apoptosis pathway to cause

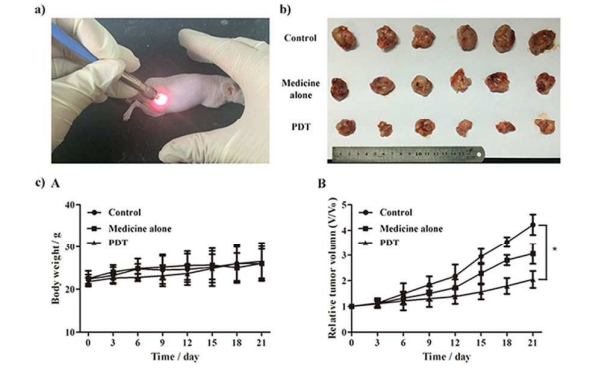

Fig. 3 Photodynamic therapy *in vivo*. a) Irradiation manner; b) Photographs of tumors collected from different groups of mice 21 day after the treatment. c) Cancer therapy in A375 tumor bearing mice *in vivo*. (A) Body weight of mice during the treatment days. (B) Changes in the relative tumor volume (n = 6) after different phototherapies. All the data above are presented as mean ± S.D. (n = 3 per group). Significant differences are considered as *$p< 0.05$; **$p< 0.01$; ***$p< 0.001$.

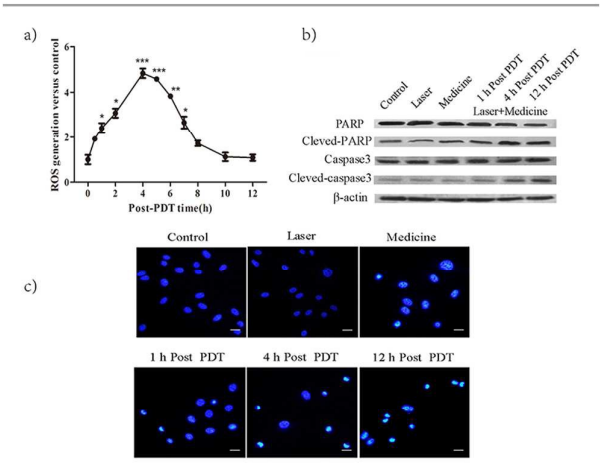

Fig. 4 The confirmatory trials of **1a**-PDT. a) The time-dependent ROS generation after PDT. All the data were presented as mean ± S.D. (n = 3 per group). b) Western blot assays of **1a**-PDT on expression of PARP, cleaved-PARP, Caspase 3 and cleaved-Caspase 3. β-actin was used as a loading control. c) Hoechst 33342 staining of nuclei in **1a**-treated and untreated cells. The cells were observed by a fluorescence microscope. Bars: 10 μm.

cell death.

In summary, we have developed a new thio-heterocyclic fused naphthalimide **1a** with brilliant fluorescent properties and photodynamic abilities. From *in vitro* experiments, **1a** exhibits not only effective phototoxicity and negligible dark toxicity in several cancer cell lines, but also excellent imaging efficacy for therapeutic process. And *in vivo* experiments on nude mice indicated that **1a**-induced PDT can suppress tumor cell proliferation after light irradiation, while basically no side effect is observed during the treatment. Additionally, taking advantage of its fluorescent behaviour, we further reveal a possible apoptosis process of **1a**-PDT treatment by mitochondrial apoptosis pathway. These results demonstrate that **1a,** as a small single-molecular theranostic candidate with stable structure, bright imaging and effective PDT, displays great potential in designing new strategies of photosensitive compounds for theranostic applications.

Live Subject Statement

All six-weeks old nude mice with half males and half females were purchased from Shanghai Slac Laboratory Animal Co. Ltd (The license of experimental animal: SCXK(shanghai) 2012-0002). The mice were maintained under the 12 hour light/dark cycles condition in the specific pathogen free (SPF) cleanroom with fresh air (more than 50%), appropriate temperature (22-26 ^{o}C) and humidness (40%-60%). The mice were freely fed with enough sterilized water and food bought from Shanghai Slac Laboratory Animal Co. Ltd. All materials and containers were disinfected and sterilizated before use.

For subcutaneous implantation, the mice were anesthetized with pelltobarbitalum natricum before injection of 1×10^{6} A375 cells. During the treatment, the mice were also nurtured in the same environment as above. After the 21 days of treatment, the mice were anesthetized and euthanasia in accordance with the international ethical standards.

All experimental procedures involving animals in this study were reviewed and approved by the institution of ethics committee in ECUST and strictly conducted according to the guidelines of Care and Use of Laboratory Animals of China (GB14925-2001) for animal experimentation.

Acknowledge

This work is financially supported by the National Natural Science Foundation of China (Grants 21236002), the National High Technology Research and Development Program of China (863 Program 2011AA10A207) and the Fundamental Research Funds for the Central Universities.

Notes and references

1. (a) N. Crawley, M. Thompson and A. Romaschin, *Anal. Chem.*, 2014, **86**, 130-160; (b) S. S. Kelkar and T. M. Reineke, *Bioconjugate Chem.*, 2011, **22**, 1879-1903.
2. (a) Y. Cho, H. Kim and Y. Choi, *Chem. Commun.*, 2013, **49**, 1202-1204; (b) S. Lee, J. Xie and X. Chen, *Chem. Rev.*, 2010, **110**, 3087-3111; (c) L. Li, Y. Liu, P. Hao, Z. Wang, L. Fu, Z. Ma and J. Zhou, *Biomaterials*, 2015, **41**, 132-140; (d) Y. Yuan, G. Feng, W. Qin, B. Z. Tang and B. Liu, *Chem. Commun.,* 2014, **50**, 8757-8760.
3. (a) Y. Yuan, R. T. K. Kwok, B. Z. Tang and B. Liu, *J. Am. Chem. Soc.*, 2014, **136**, 2546-2554; (b) R. Kumar, W. S. Shin, K. Sunwoo, W. Y. Kim, S. Koo, S. Bhuniya and J. S. Kim, *Chem. Soc. Rev.*, 2015, **44**, 6670-6683; (c) R. Kumar, J. Han, H. J. Lim, W. X. Ren, J. Y. Lim, J. H. Kim and J. S. Kim, *J. Am. Chem. Soc.*, 2014, **136**, 17836-17843; (d) J. Kim, C. H. Tung and Y. Choi, *Chem. Commun.*, 2014, **50**, 10600-10603; (e) S. Bhuniya, S. Maiti, E. J. Kim, H. Lee, J. L. Sessler, K. S. Hong and J. S. Kim, *Angew. Chem. Int. Edit.*, 2014, **53**, 4469-4474; (f) Y. Chen, A. Gryshuk, S. Achilefu, T. Ohulchansky, W. Potter, T. Zhong, J. Morgan, B. Chance, P. N. Prasad, B. W. Henderson, A. Oseroff and R. K. Pandey, *Bioconjugate Chem.*, 2005, **16**, 1264-1274; (g) Y. Yuan, C. J. Zhang, M. Gao, R. Zhang, B. Z. Tang and B. Liu, *Angew. Chem., Int. Ed.*, 2015, **54**, 1780-1786.
4. (a) E. A. Sykes, J. Chen, G. Zheng and W. C. Chan, *ACS nano*, 2014, **8**, 5696-5706; (b) A. Senpan, S. D. Caruthers, I. Rhee, N. A. Mauro, D. Pan, G. Hu, M. J. Scott, R. W. Fuhrhop, P. J. Gaffney, S. A. Wickline and G. M. Lanza, *ACS nano*, 2009, **3**, 3917-3926; (c) S. Nie, *Nanomedicine*, 2010, **5**, 523-528; (d) S. Luo, X. Tan, Q. Qi, Q. Guo, X. Ran, L. Zhang, E. Zhang, Y. Liang, L. Weng, H. Zheng, T. Cheng, Y. Su and C. Shi, *Biomaterials*, 2013, **34**, 2244-2251.
5. (a) X. Tan, S. Luo, D. Wang, Y. Su, T. Cheng and C. Shi, *Biomaterials*, 2012, **33**, 2230-2239; (b) J. F. Lovell, T. W. Liu, J. Chen and G. Zheng, *Chem. Rev.*, 2010, **110**, 2839-2857; (c) S. Erbas-Cakmak and E. U. Akkaya, *Angew. Chem. Int. Edit.*, 2013, **52**, 11364-11368; (d) J. P. Celli, B. Q. Spring, I. Rizvi, C. L. Evans, K. S. Samkoe, S. Verma, B. W. Pogue and T. Hasan, *Chem. Rev.*, 2010, **110**, 2795-2838; (e) S. K. Pandey, A. L. Gryshuk, M. Sajjad, X. Zheng, Y. Chen, M. M. Abouzeid, J. Morgan, I. Charamisinau, H. A. Nabi, A. Oseroff and R. K. Pandey, *J. Med. Chem.*, 2005, **48**, 6286-6295; (f) E. Zhao, H. Deng, S. Chen, Y. Hong, C. W. T. Leung, J. W. Y. Lam and B. Z. Tang, *Chem. Commun.*, 2014, **50**, 14451-14454.
6. S. Singh, A. Aggarwal, N. V. S. D. K. Bhupathiraju, G. Arianna, K. Tiwari and C. M. Drain, *Chem. Rev.*, 2015, **115**, 10261-10306.
7. (a) Q. Zou, H. Zhao, Y. Zhao, Y. Fang, D. Chen, J. Ren, X. Wang, Y. Wang, Y. Gu and F. Wu, *J. Med. Chem.*, 2015, **58**, 7949-7958; (b) J. Liu, Y. Chen, G. Li, P. Zhang, C. Jin, L. Zeng, L. Ji and H. Chao, *Biomaterials*, 2015, **56**, 140-153; (c) A. Kamkaew, S. H. Lim, H. B. Lee, L. V. Kiew, L. Y. Chung and K. Burgess, *Chem. Soc. Rev.*, 2013, **42**, 77-88; (d) S. D. Topel, G. T. Cin and E. U. Akkaya, *Chem. Commun.*, 2014, **50**, 8896-8899.
8. (a) H. Yu, Y. Xiao and L. Jin, *J. Am. Chem. Soc.*, 2012, **134**, 17486-17489; (b) M. Lv and H. Xu, *Curr. Med. Chem.*, 2009, **16**, 4797-4813; (c) T. Guo, L. Cui, J. Shen, R. Wang, W. Zhu, Y. Xu and X. Qian, *Chem. Commun.*, 2013, **49**, 1862-1864; (d) L. Ingrassia, F. Lefranc, R. Kiss and T. Mijatovic, *Curr. Med. Chem.*, 2009, **16**, 1192-1213.
9. (a) S. Banerjee, E. B. Veale, C. M. Phelan, S. A. Murphy, G. M. Tocci, L. J. Gillespie, D. O. Frimannsson, J. M. Kelly and T.

Gunnlaugsson, *Chem. Soc. Rev.*, 2013, **42**, 1601-1618; (b) S. Tan, H. Yin, Z. Chen, X. Qian and Y. Xu, *Eur. J. Med. Chem.*, 2013, **62**, 130-138; (c) X. Wang, Z. Chen, L. Tong, S. Tan, W. Zhou, T. Peng, K. Han, J. Ding, H. Xie and Y. Xu, *Eur. J. Med. Chem.*, 2013, **65**, 477-486; (d) L. Cui, Z. Peng, C. Ji, J. Huang, D. Huang, J. Ma, S. Zhang, X. Qian and Y. Xu, *Chem. Commun.,* 2014, **50**, 1485-1487.

10. (a) A. Gorman, J. Killoran, C. O'Shea, T. Kenna, W. M. Gallagher and D. F. O'Shea, *J. Am. Chem. Soc.*, 2004, **126**, 10619-10631; (b) S. Ozlem and E. U. Akkaya, *J. Am. Chem. Soc.*, 2009, **131**, 48-49; (c) Y. Yang, Q. Guo, H. Chen, Z. Zhou, Z. Guo and Z. Shen, *Chem. Commun.*, 2013, **49**, 3940-3942; (d) T. Yogo, Y. Urano, Y. Ishitsuka, F. Maniwa and T. Nagano, *J. Am. Chem. Soc.*, 2005, **127**, 12162-12163.
11. J. C. Koziar and D. O. Cowan, *Accounds. Chem. Res.*, 1978, **11**, 334-341.
12. (a) Y. Xu, B. Qu, X. Qian and Y. Li, *Bioorg. Med. Chem. Lett.*, 2005, **15**, 1139-1142; (b) X. Qian, Y. Li, Y. Xu, Y. Liu and B. Qu, *Bioorg. Med. Chem. Lett.*, 2004, **14**, 2665-2668.
13. M. Ethirajan, Y. Chen, P. Joshi and R. K. Pandey, *Chem. Soc. Rev.*, 2011, **40**, 340-362.
14. B. R. Singh, B. N. Singh, W. Khan, H. B. Singh and A. H. Naqvi, *Biomaterials*, 2012, **33**, 5753-5767.
15. K. M. Boatright and G. S. Salvesen, *Curr. Opin. Cell. Biol.*, 2003, **15**, 725-731.

One Small Molecule as Theranostic Agent: Naphthalimide Dye for Subcellular Fluorescent Localization and Photodynamic Therapy *in vivo*

Lei Zhang,[a,‡] Kecheng Lei,[b,‡] Jingwen Zhang,[a] Wenlin Song,[a] Yuanhong Zheng,[b] Shaoying Tan,[a] Yuwei Gao,[b] Yufang Xu,[a,*] Jianwen Liu[b,*] and Xuhong Qian[a,*]

A small single-molecule theranostic agent based on naphthalimide was developed, which possessed both bright fluorescent imaging and effective photodynamic therapeutic treatment.